Predicted and Measured Response of an Integral Abutment Bridge

Jolene L. Fennema[1]; Jeffrey A. Laman, P.E.[2]; and Daniel G. Linzell, P.E.[3]

Abstract: This project examined several uncertainties of integral abutment bridge design and analysis through field-monitoring of an integral abutment bridge and three levels of numerical modeling. Field monitoring data from a Pennsylvania bridge site was used to refine the numerical models that were then used to predict the integral abutment bridge behavior of other Pennsylvania bridges of similar construction. The instrumented bridge was monitored with 64 gages; monitoring pile strains, soil pressure behind abutments, abutment displacement, abutment rotation, girder rotation, and girder strains during construction and continuously thereafter. Three levels of numerical analysis were performed in order to evaluate prediction methods of bridge behavior. The analysis levels included laterally loaded pile models using commercially available software, two-dimensional (2D) single bent models, and 3D finite element models. In addition, a weather station was constructed within the immediate vicinity of the monitored bridge to capture environmental information including ambient air temperature, solar radiation, wind speed and direction, humidity, rainfall, and barometric pressure. Laterally loaded pile models confirmed that inclusion of multilinear soil springs created from *p-y* curves is a valid approach for modeling soil–pile interaction within a finite element program. The 2D and 3D numerical models verified the field data indicating that primary accommodation of superstructure expansion and contraction is through rotation of the abutment about its base rather than longitudinal translation, as assumed in the original design of this bridge. Girder axial forces were suspected to be influenced by creep and shrinkage effects in the bridge superstructure. Pile strains were found to be well below strains corresponding to pile plastic moment. Overall, the 2D numerical model and the 3D numerical model predicted very similar behavior.

DOI: 10.1061/(ASCE)1084-0702(2005)10:6(666)

CE Database subject headings: Bridge abutments; Monitoring; Responses; Integrals; Measurement; Predictions.

Introduction

With the construction success of integral abutment (IA) bridges, overall IA bridge lengths have increased. However, the design of IA bridges of all lengths remains largely empirically based. In addition, IA bridge performance problems have arisen due to differences in IA detailing philosophy and bridge construction methods. A major study (Oesterle et al. 1998) conducted under the sponsorship of the Federal Highway Administration (FHWA) identified several uncertainties in the prediction of long- and short-term behavior of IA bridges, including: effects of annual temperature variation and internal restraint and thermal mass; effects of diurnal temperature movement; effective coefficient of thermal expansion; effects of creep and shrinkage on thermal expansion; foundation stiffness, particularly the relationship between passive earth pressure and abutment movement and the capacity of the abutment piles to accommodate movement; and stiffness and load transfer through the piers. These uncertainties, coupled with the number of issues encountered during IA bridge design including: pile orientation, pile size, pile depth, pile predrill, soil modeling, approach slab influence, backfill, total movement under design temperature range, girder fixity, girder rotation, abutment rotation, stresses in girders, stresses at pile–abutment connection, down drag of piles, and coefficient of thermal expansion for concrete combine to create a very complicated process.

The present study examined several uncertainties typical of IA bridge design and construction through field monitoring and numerical modeling of a recently constructed integral abutment bridge in Pennsylvania. This paper is a condensation of a larger study reported by Fennema (2003). The study bridge reflects standard IA design and construction in the state of Pennsylvania. Refinement of the numerical models was conducted based on field data and used to predict integral abutment bridge behavior. To better predict the behavior of IA bridges, this study focused on the following aspects: use of commercially available pile analysis tools and *p-y* curves in predicting laterally loaded pile behavior; effect of soil stiffness on pile behavior through numerical modeling of linear and multilinear soil springs; effect of predrilled holes filled with loose sand on pile behavior; and influence of integral abutments on longitudinal bridge stresses.

[1]Fabcon East, LLC, 5100 Tilghman St., Ste. 155, Allentown, PA 18104. E-mail: jolene.fennema@fabcon-usa.com

[2]Associate Professor of Civil Engineering, Dept. of Civil and Environmental Engineering, The Pennsylvania State Univ., 212 Sackett Building, University Park, PA 16802 (corresponding author). E-mail: jlaman@engr.psu.edu

[3]Associate Professor of Civil Engineering, Dept. of Civil and Environmental Engineering, The Pennsylvania State Univ., 212 Sackett Building, University Park, PA 16802. E-mail: dlinzell@engr.psu.edu

Note. Discussion open until April 1, 2006. Separate discussions must be submitted for individual papers. To extend the closing date by one month, a written request must be filed with the ASCE Managing Editor. The manuscript for this paper was submitted for review and possible publication on December 8, 2003; approved on October 15, 2004. This paper is part of the ***Journal of Bridge Engineering***, Vol. 10, No. 6, November 1, 2005. ©ASCE, ISSN 1084-0702/2005/6-666–677/$25.00.

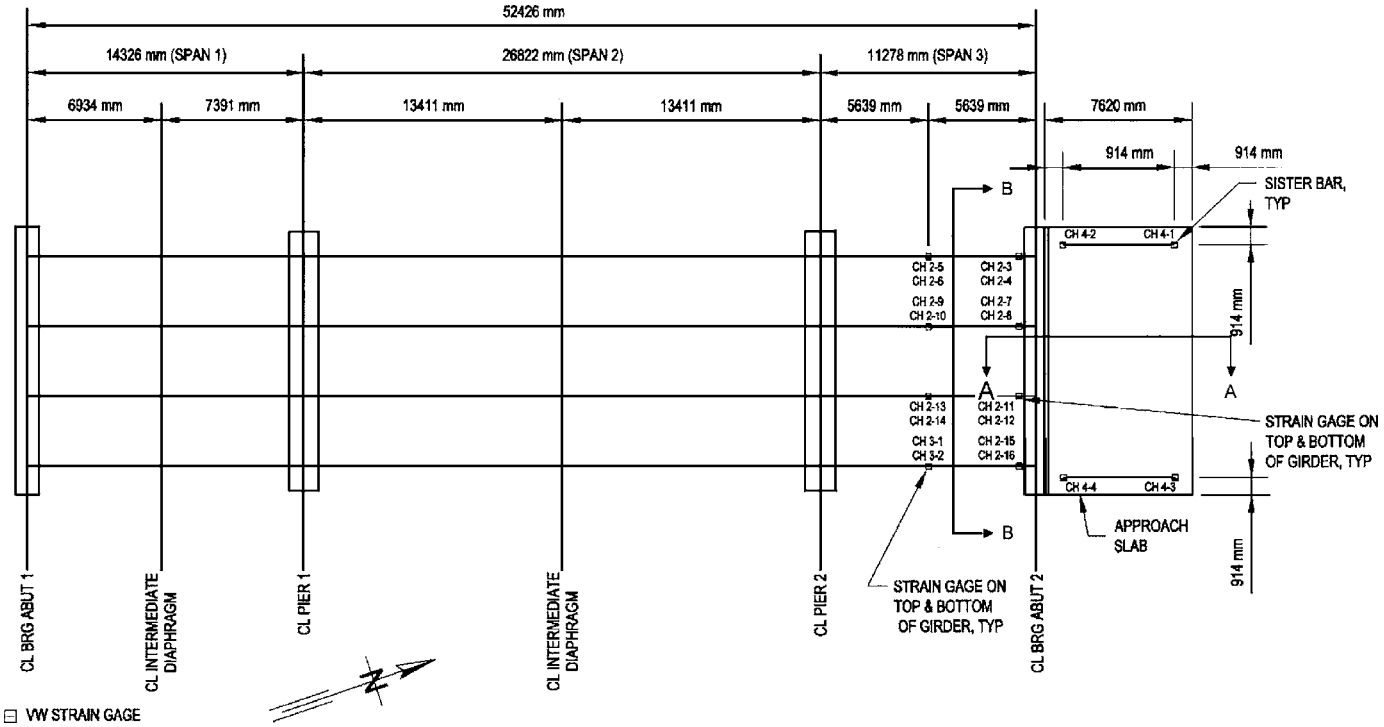

Fig. 1. Bridge plan view and instrument location

Bridge Description and Monitoring

The monitored IA bridge is a three-span, composite structure with four prestressed, concrete I-girders bearing on reinforced concrete piers and abutments with spans of 14,330, 26,820, and 10,670 mm. The bulb-tee girders were cast during March, 2002 and are spaced at 3,594 mm, cast integrally with abutments, and support a 230 mm concrete deck (see Figs. 1, 2, and 3). Piers are designed as semirigid self-supporting substructures with 70 mm elastomeric bearing pads that allow longitudinal movement of the superstructure. The south abutment and south girder ends are fixed against translation and rotation (no expansion joint) and the abutment bears directly on rock. The north abutment is a standard Pennsylvania Dept. of Transportation integral abutment, 4,390 mm average height from bottom of abutment to bottom of girder. The abutment is supported by a single row of eight HP 12×74 piles with weak axis orientation, embedded 610 mm into the abutment, and driven to refusal (see Fig. 2). A 25 mm thick extruded polystyrene insulation sheet separates the south abutment from the overly graded subgrade material to reduce backfill passive soil pressure. 7,620 mm long by 460 mm thick reinforced concrete approach slabs are to be constructed at both ends of the bridge in the future. A 50 mm thick extruded polystyrene insulation sheet separates the abutment from the wing walls to isolate component movements.

North abutment piles were driven June 27, 2002 through brown, weathered shale fill in an approximately 3,050 mm deep, predrilled hole. Loose sand was placed in each predrilled hole prior to driving, however, the sand was compacted significantly during pile driving. The top 1,200–1,500 mm of the predrilled hole was filled with loose sand at each location at the completion of pile driving. Due to the compaction of the sand, it was expected that predrilled holes will provide very limited allowance for pile displacement, therefore, the sand was neglected in the numerical models.

Placement of the bridge deck was North to South with intermediate diaphragms and continuity diaphragms being placed simultaneously with the deck. The backwall of the north abutment was placed 2 days later. Girders and north abutment were instrumented with tiltmeters on October 8, 2002.

Instrumentation Plan

The instrumentation plan was developed based on an initial numerical analysis that is discussed in detail by Fennema (2003). Electronic transducers were attached to the bridge to monitor pressures, strains, displacements, and relative tilting angles. A weather station was constructed within 100 m of the bridge to monitor climatic and environmental conditions such as wind speed, wind direction, relative humidity, barometric pressure, ambient air temperature, solar radiation, and precipitation.

Figs. 1, 2, and 3 present the instrumentation plan for the bridge. Sixty vibrating wire based instruments were installed on the bridge consisting of 46 surface-mounted strain gages, three pressure cells, three extensometers, and eight tiltmeters. A total of 30 strain gages were mounted on two of the eight piles. Strain gages mounted on each of the two piles include three sets of three gages to measure bending and axial strain and six single gages to measure axial strain only. The gages placed in sets of three were located just below the abutment, between the abutment and predicted point of maximum moment, and at the predicted point of maximum moment. The remaining individual gages were attached to the center of gravity at even intervals between the estimated point of fixity for the pile and the pile tip. Strain gages mounted on the prestressed concrete girders were located at the

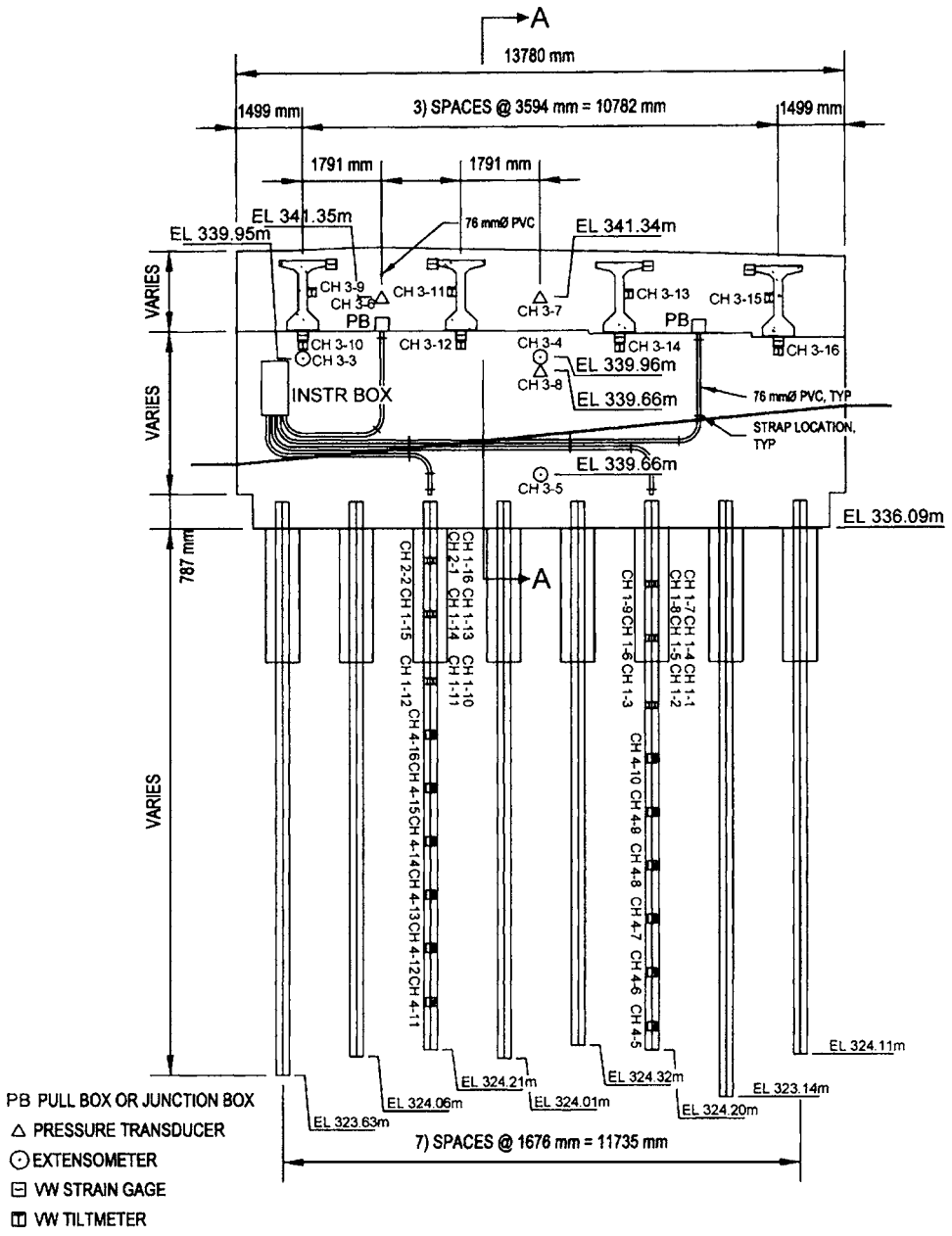

Fig. 2. Bridge north abutment view and instrument location

center of the north span and 1 in. from the north abutment. Each location has one gage placed at the middle of the bottom flange and another gage placed on the side of the top flange for a total of 16 gages. These locations returned measurement of major axis bending and girder axial force. Three borehole extensometers were placed to monitor abutment longitudinal translation and indirectly, abutment rigid body rotation about a transverse horizontal axis, and a vertical axis. North abutment longitudinal movement and three axis of rotation were monitored. The pressure cells were placed higher on the abutment to concentrate the readings directly behind the girders. Recent studies have shown pressure to only exist in that area (Lawver et al. 2000). Tiltmeters were installed on the north abutment to verify rotations calculated from extensometer readings and north span girders. Four additional tiltmeters were mounted to the web of each girder at the north abutment to observe the rotational restraint of the diaphragm by comparing rotations between girders and abutment.

Numerical Models

Three levels of numerical analysis were employed to determine the movements and behavior of integral abutment bridges due to thermal loads. Level 1 is an analysis of the behavior of the laterally loaded piles alone with no abutment or superstructure. This analysis required the development of soil springs properties through a commercially available pile analysis program and by generating *p-y* curves. Level 2 analysis [Fig. 4(a)] consists of a two-dimensional, three-bent numerical model developed using *STAAD Pro* composed of frame members and soil springs. This model is representative of a typical numerical model commonly developed for design. Level 3 analysis [Fig. 4(b)] utilizes a three-dimensional (3D) finite element model developed in *STAAD Pro* consisting of frame members, plate elements, and soil springs. The 3D model is considerably more complex and was expected to provide a more accurate prediction of movements and stresses.

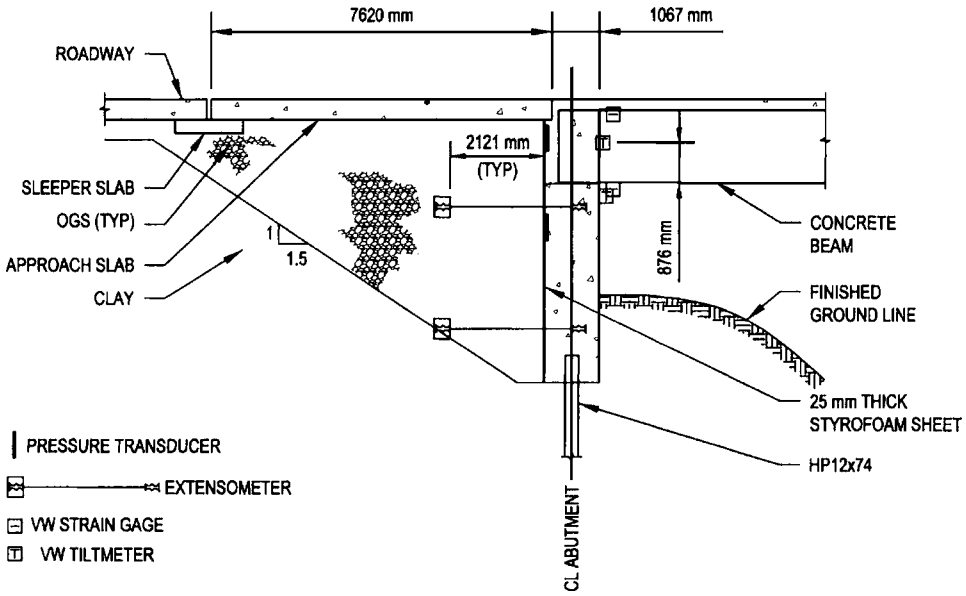

Fig. 3. Bridge abutment section and instrument location

The initial models of each level of analysis provided an uncalibrated prediction of integral abutment bridge movements and behavior. They were later adjusted, based on field data and concrete material test information to provide a more accurate prediction of bridge behavior.

Level 1: Laterally Loaded Pile Model

Three laterally loaded pile models were developed to determine the validity of using multilinear soil springs: (1) a series of 305 mm long beam elements with multilinear soil springs applied at each node using a commercially available structural analysis program; (2) pile analysis software *COM624P* (Wang and Reece 1993); and (3) a series of 305 mm long beam elements with linear soil springs, the stiffness of which was derived from *COM624P*. Each model consists of a single HP 12×74 pile oriented for weak axis bending with an applied 645 kN axial dead load and an applied lateral load chosen to develop pile plastic moment capacity. Boundary conditions in all three models consisted of fixed rotation and free translation at the pile head and fixed translation and free rotation at the pile tip.

Development of Soil Springs

The most common method of determining soil spring stiffness for a structural numerical model employs *COM624P*, software distributed by the FHWA. This method is iterative and relatively cumbersome. Alternatively, *p-y* curves and nonlinear theories of soil mechanics can be employed as a more direct method of determining soil spring stiffness. Finally, dynamic soil testing at the bridge site can be employed, however, this is not normally practical.

COM624P is widely used for IA bridge design, however, it requires an iterative process between *COM624P* and a commercially available structural analysis program until forces and deflections are balanced between the two programs. Typically *COM624P* models a fixed-head condition and a lateral force applied until the plastic moment capacity of the pile is reached. The initial deflection is then compared to the assumed design deflection to evaluate the movement demand and the elastic or plastic response to determine appropriate structural analysis of the bridge. Linear soil spring stiffness is determined from *COM624P* results and incorporated into a bridge analysis model, where the lateral force is obtained. Iterations between the lateral force applied in *COM624P* and the linear soil springs in the numerical model continue until both models converge.

p-y curves can be used to establish approximating multilinear soil springs. The present study followed the method described in the FHWA "Behavior of piles and pile groups under lateral load" (Reese 1985). For a laterally loaded pile, the soil modulus (E_s) is defined as p (load) divided by y (displacement) with units of force per length squared. A representative *p-y* curve at a certain depth is shown in Fig. 5 with approximating multilinear spring stiffnesses superimposed. Multilinear spring stiffnesses are developed through a sequence of linear regressions to fit *p-y* curves at depths corresponding to locations of soil springs defined in the bridge structural analysis model. These multilinear spring stiffnesses are then provided as input to the bridge structural analysis model along the pile length.

Level 2: Two-Dimensional Single Bent Model

The IA bridge 2D numerical model developed for this study is a modified version of the original bridge design model composed entirely of beam and multilinear spring elements. The four prestressed concrete girders and reinforced concrete deck slab properties are lumped into one beam element located at the positive bending elastic neutral axis with rigid offsets for the element from the abutments and piers. Each reinforced concrete abutment is composed of a single beam element. The eight steel piles are lumped into a single pile modeled as a series of 305 mm long beam elements with multilinear soil springs at each node along the depth. Both piers are modeled as a single beam element with a 76 mm long beam element to represent elastomeric bearings.

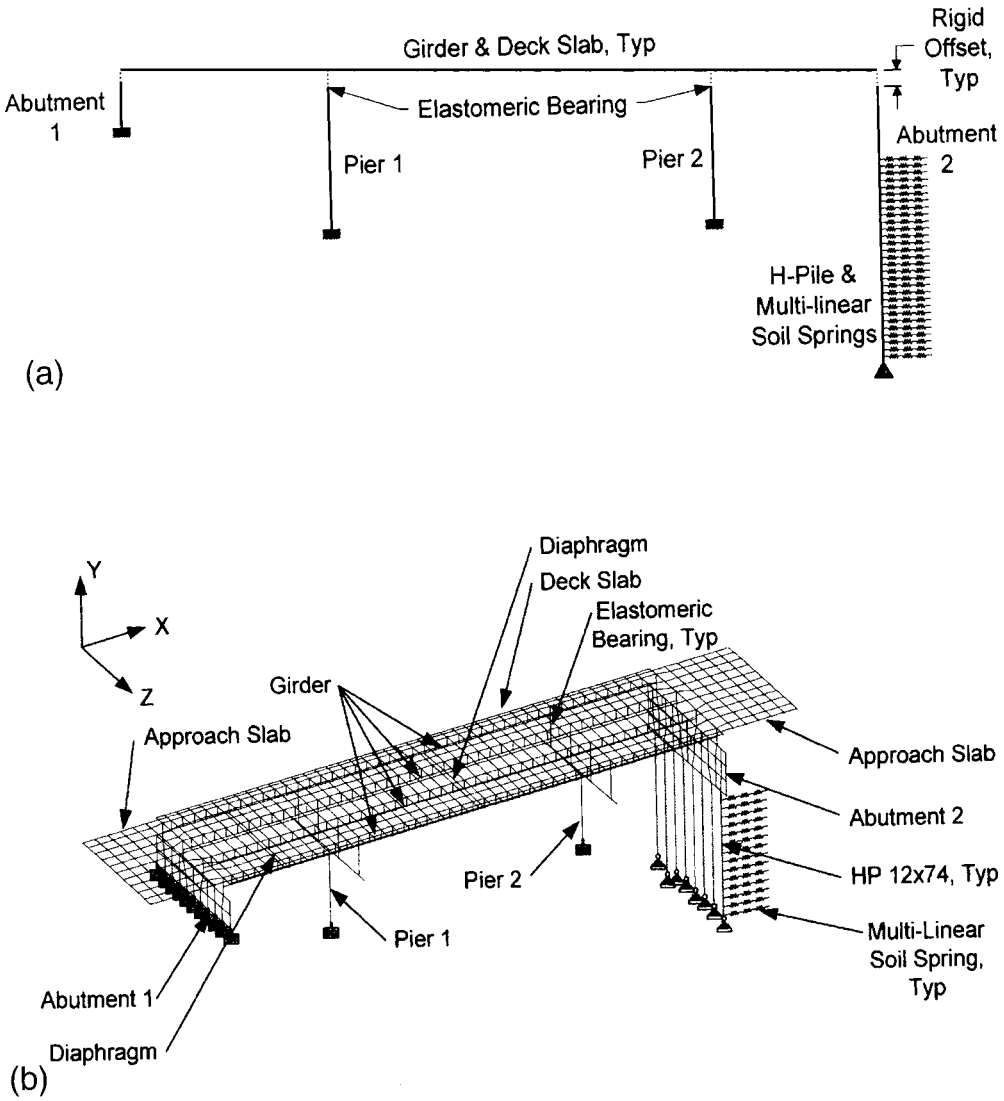

Fig. 4. Levels 2 and 3 numerical models

The south abutment is fixed against rotation and translation. The pile tip is translationally fixed (driven to refusal) and rotationally free. There are no soil springs behind the backwall of the north abutment, assuming the 25 mm layer of extruded polystyrene relieves passive soil pressure. The base of Piers 1 and 2 are fixed against rotation and translation. Load for the model consists of ±44°C applied to each span of the superstructure with the coefficient of thermal expansion (α) taken as $10.8 \times 10^{-6}/°F$ (AASHTO 1989).

Level 3: Three-Dimensional Finite Element Model

The three-dimensional bridge model is composed of beam and plate elements. The four prestressed concrete girders and intermediate and continuity diaphragms are modeled with beam elements. The bridge deck, abutments and approach slabs are modeled with plate elements. Piles and piers are modeled with beam elements. Elastomeric bearings are modeled as 3 in. long beam elements as in the 2D model. The south abutment element support boundaries are restrained against rotation and translation at each node of the plate elements. North abutment pile support boundaries are fixed against translation. The north abutment is not restrained by soil springs due to a 25 mm thick extruded polystyrene between it and the backfill, designed to relieve passive soil pressure. Piers are fixed against rotation and translation at the base. Girders are rigidly connected at both abutments and supported on elastomeric bearings through a rigid link. The loading, as in the Level 2 analysis is a ±44°C load to girders, deck, and approach slab element.

Discussion of Results

Field data were collected at the bridge and weather station between November, 24 2002 and March 24, 2003. This period represents the first contraction cycle of the bridge. The field data were reduced to extract girder axial force, girder rotation, abutment displacement, abutment rotation, abutment soil pressure, and pile moment due to temperature load only.

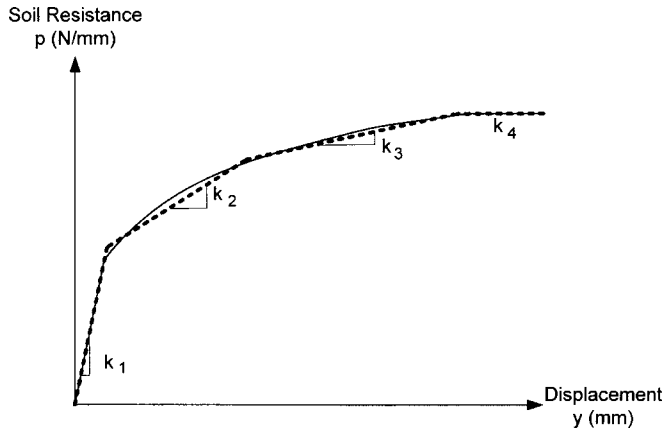

Fig. 5. Multilinear soil spring approximation of *p-y* relationship

Soil–Pile Interaction

Numerical, pile models incorporating multilinear soil springs, developed from *p-y* curves to include soil–pile interaction were compared to two HP 12×74 pile models oriented for weak axis bending. The first pile model consists of a laterally loaded pile evaluated using *COM624P* and the second is a finite element model incorporating linear soil springs with stiffness derived from soil resistance calculated by *COM624P*. Results (see Fig. 6) indicate that the linear soil spring pile model and *COM624P* compare closely as expected due to the direct calibration between the two models. Moment and displacement response of the multilinear soil spring pile model compares well with the other two pile models. Pile–head displacement of the multilinear soil spring pile model differs from *COM624P* by 7.5%. The distance to inflection point is greater in the multilinear soil spring

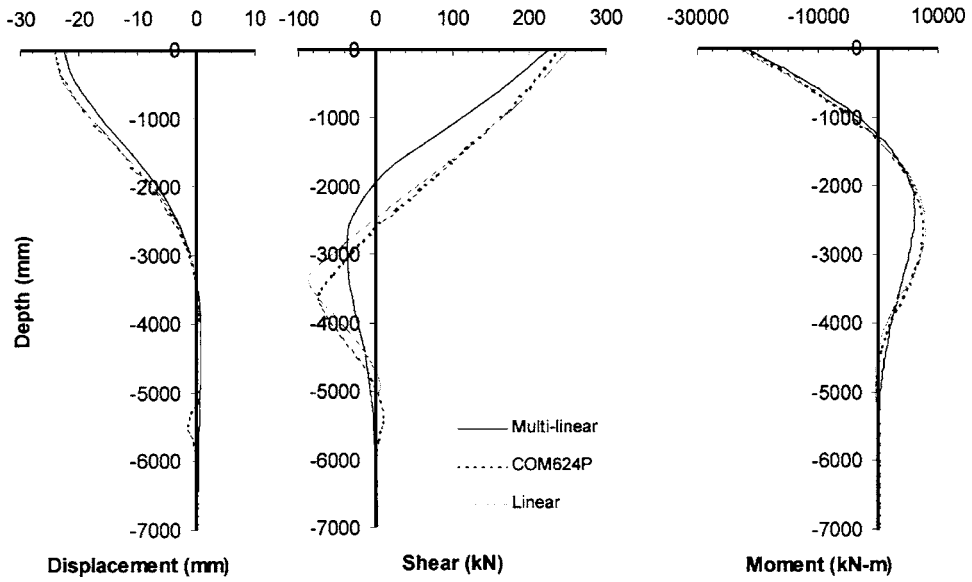

Fig. 6. Comparison of numerical model with multilinear soil springs to *COM624P* and linear

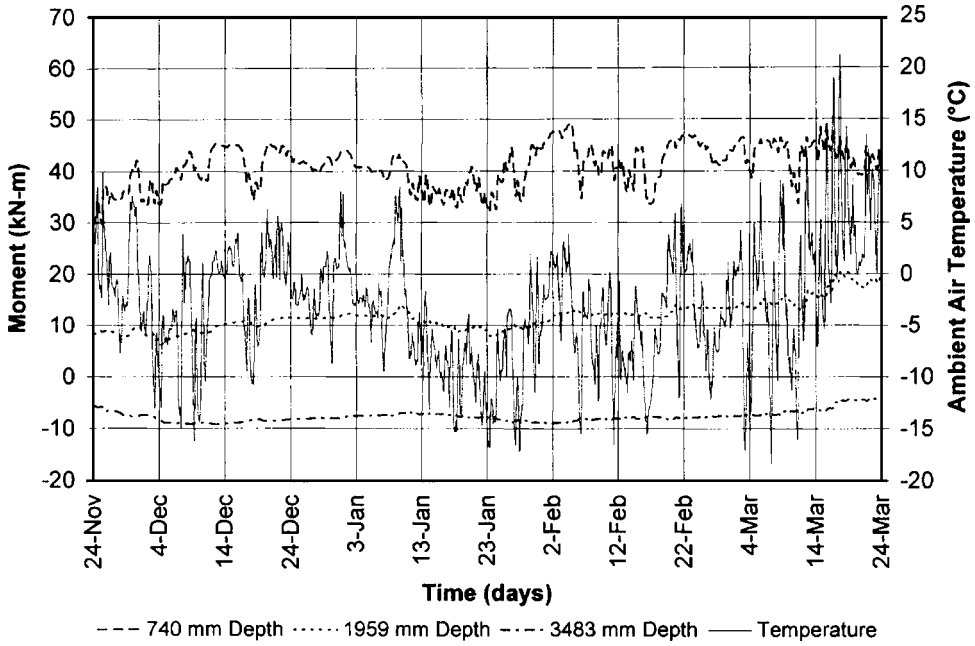

Fig. 7. Measured bridge pile bending moment for pile 3 with temperature

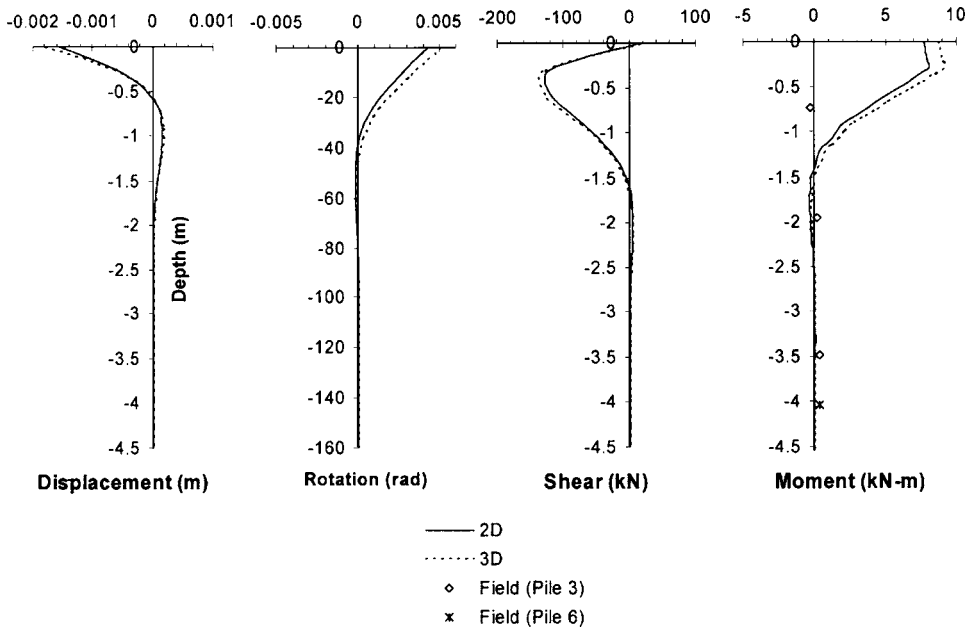

Fig. 8. Bridge response under design contraction temperature load

pile model than *COM624P* by approximately 30%. Maximum moment within this distance differs from the *COM624P* pile model by 17%. Depth to maximum moment from the pile head is shallower in the multilinear soil spring pile model than *COM624P* by 10%. Depth to the point of fixity differs from the *COM624P* pile model by 23%. Shear at the pile head of each model is similar with the multilinear soil spring pile model being less than *COM624P* by 6%.

COM624P is used as a basis for comparison as it is widely accepted and was developed based on numerous tests of in situ piles (Wang and Reece 1993). Pile response differences between the numerical pile models and *COM624P* are primarily attributed to modeling differences. Numerical models consider the actual shape of the pile and evaluate the soil–pile interaction using the direct stiffness method, whereas *COM624P* assumes a circular pile and solves the problem using an equilibrium formulation.

Measured and Predicted Pile Behavior

Fig. 7 presents field data for pile bending moment due to superstructure thermal expansion and contraction at three depths for Pile 3 of the bridge. The top of pile corresponds to the bottom of

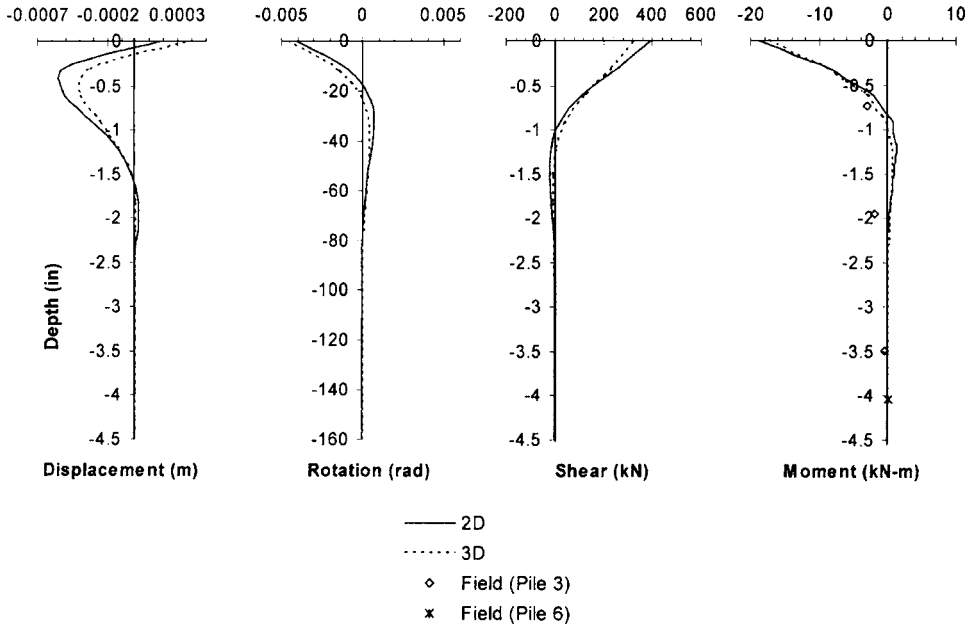

Fig. 9. Bridge response under design expansion temperature load

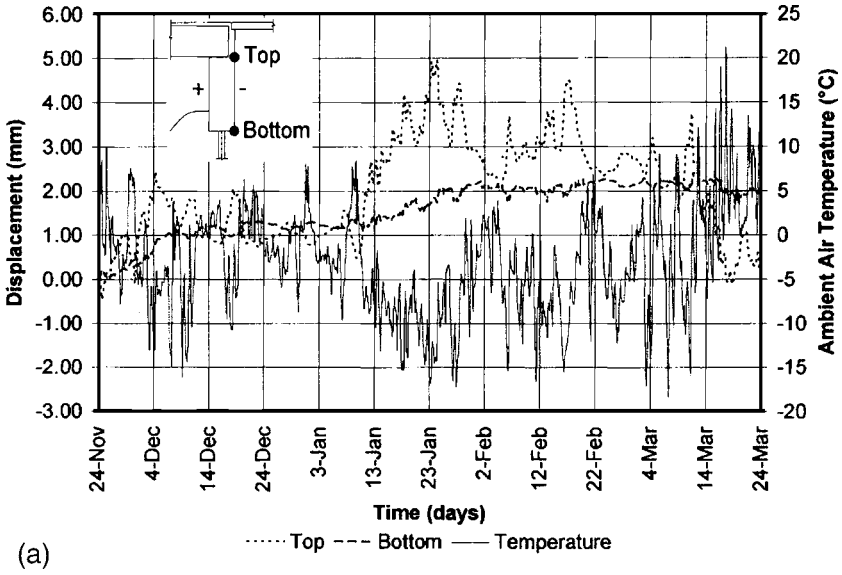

Fig. 10. Measured north abutment (a) displacement, top and bottom with temperature and (b) rotation with temperature

abutment at a depth of 0.0 mm. Fig. 7 indicates that moment near the pile head is greater than other points along the pile. In addition, there is a point of zero moment between a depth of 1,960 and 3,480 mm. The largest moment recorded is 49 kN m when the ambient air temperature was 14°C.

Dynamic soil testing (Fennema 2003) of the brown, weathered, shale fill used at the site was conducted at the bridge during Spring 2002. The dynamic soil testing identified initial soil stiffness and was used to calibrate the multilinear soil spring initial stiffness incorporated into Level 1 and 2 numerical models. To compare the 2D pile model response with the 3D pile model response and the measured response of piles, the displacement, rotation, shear, and moment response of the eight piles modeled in the 3D model and the measured response were averaged (2D models all eight piles together in one). Reduced field data of the north abutment piles consist of moments only due to the type and location of the gages. This field data was extrapolated (Fennema 2003) to estimate pile moments resulting from a design ±4 °C temperature change. A majority of abutment strain data collection took place under ambient air temperatures between −9 and 7°C, with a median ambient air temperature of −4 °C, therefore, extrapolation of best fit curves was employed to obtain results for comparative purposes.

Fig. 8 and 9 present measured and numerical model pile response during maximum design bridge contraction and expansion (±44 °C), respectively. The 2D and 3D average numerical results for contraction compare closely, while moments, derived from field data, differ from the numerical model results. These differences are due, in part, to the limited field data and the necessity to extrapolate field data to the ±44 °C design temperature range. It is also partially due to differences in actual and idealized soil stiffness and not modeling the fill on the bridge face of the abutment. Extrapolated measured response under bridge expansion compares more favorably with both the 2D and 3D numerical models as observed in Fig. 9.

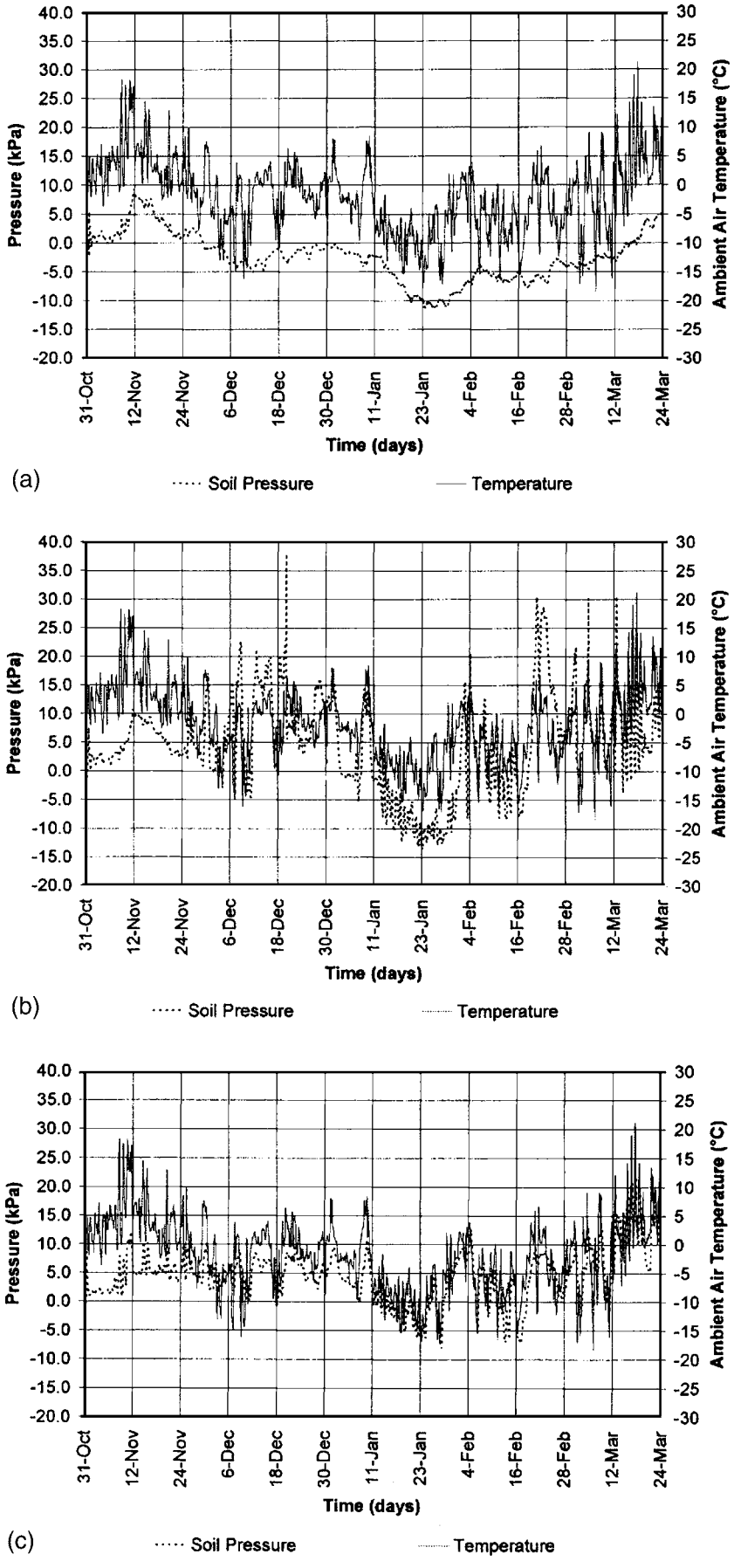

Fig. 11. North abutment pressure meter and temperature response: (a) Channel 3-6–North Abutment, west, high; (b) Channel 3-7–North Abutment, center, high; and (c) Channel 3-8–North Abutment, center, low

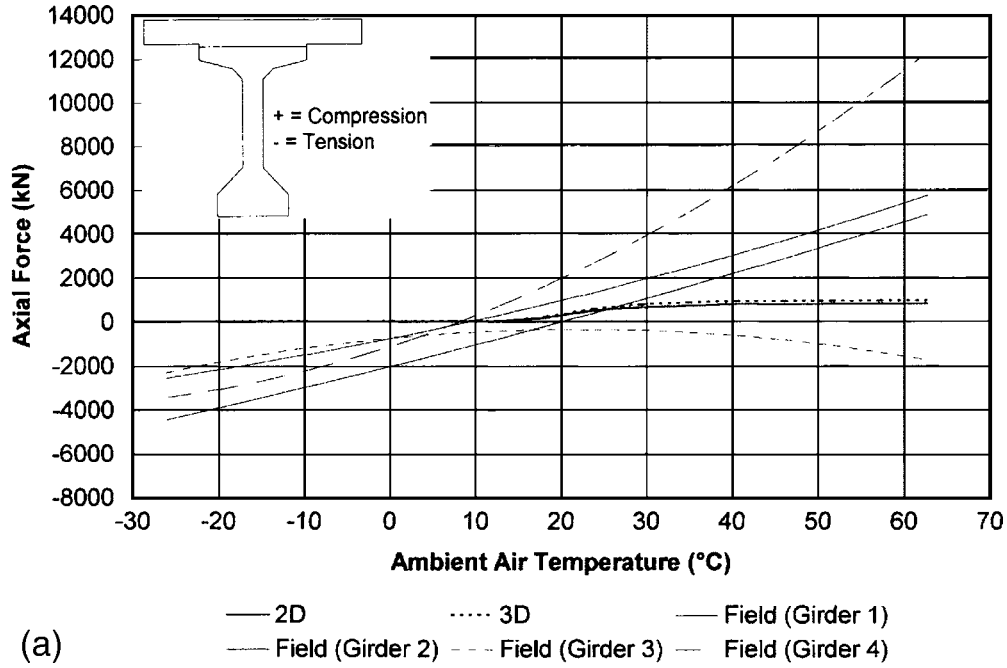

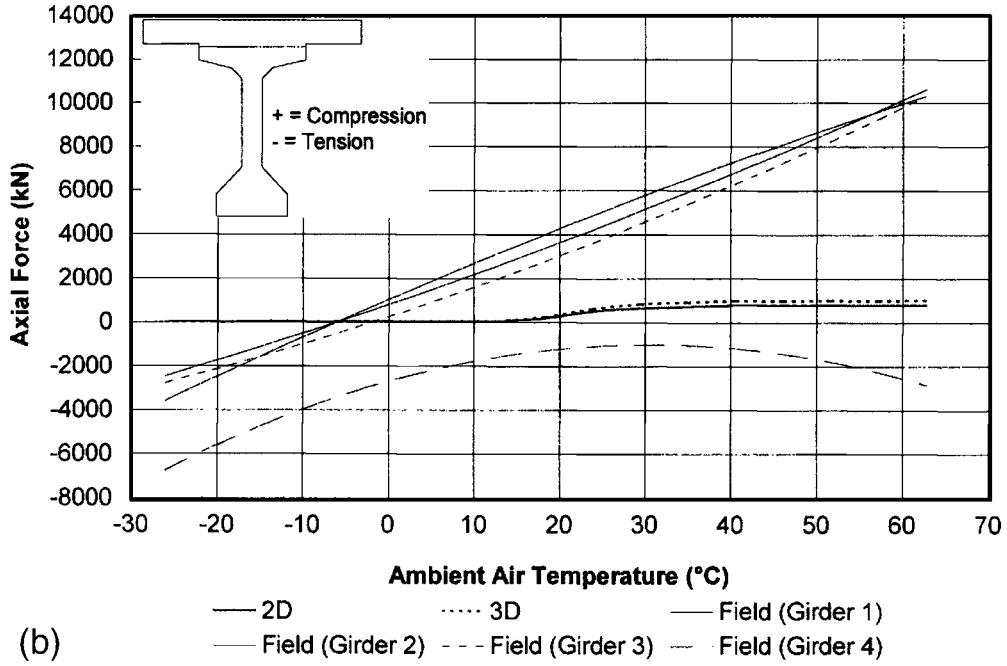

Fig. 12. Measured and predicted girder axial force at midspan (a) and abutment (b)

Abutment Movement

The IA bridges are designed to allow longitudinal displacement of the abutment piles during superstructure expansion and contraction. North abutment measured displacements [Fig. 10(a)] indicate that the primary mode of abutment movement is rotation about the abutment base rather than longitudinal abutment displacement. The base of the abutment initially displaced inward, (toward the bridge) during contraction and did not return to zero during bridge expansion. This trend was also observed by Lawver et al. (2000). In addition, under maximum measured bridge contraction, the displacement at the top of the north abutment is 4.8 mm at an ambient air temperature of −17°C Calculated thermal movement demand at −17°C, assuming an 18°C initial setting, is equal to 20 mm or a calculated abutment displacement of over four times the measured displacement.

Measured north abutment rotation is presented in Fig. 10(b). Abutment rotation is strongly correlated to the change in ambient air temperature. It can also be observed that there is approximately a 6 h lag in bridge response due to change in ambient air temperature as a result of the thermal inertia. This correlation

indicates that response is largely abutment rotation rather than purely translation. Girder flexibility and joint flexibility between the girder and abutment permit the rotation.

Abutment Soil Pressure

Three pressure transducers were installed on the north abutment on September 8, 2003. Transducers were located at the face of the abutment behind the extruded polystyrene. Fig. 11(a–c) present soil pressure data from transducers located; (a) at the mid-height between the exterior and interior girder; (b) at the mid-height between the two interior girders; and (c) 1,680 mm below pressure transducer (b). The gages were zeroed 1 day prior to backfilling on October, 31 2002. An initial increase in soil pressure due to backfilling can be observed followed by a relief in the pressure with the remaining data correlating well with ambient air temperature. Measured soil pressures fall within the range of active and at-rest soil pressures.

Fig. 11(a) indicates comparable soil pressure magnitudes with Fig. 11(b) as expected because both transducers are located at the same elevation on the abutment. The figures also indicate that soil pressure is consistently and slightly greater at location (b) than location (c). This is in agreement with work by Oesterle et al. (1998) where soil pressure was shown to be greatest at a point approximately 1/3 of the abutment height below the road surface. Difficulties with temperature compensation were experienced with the pressure transducers, resulting in reporting of some negative readings. Further research is required to establish the cause.

Girder–Abutment Connection Stiffness

Tiltmeters were attached to the abutment just below each girder and to the web of each girder near the abutment. Observation of the tiltmeter response data indicates that girders and abutment are rotating in opposite directions during bridge contraction and expansion, demonstrating that the connection is not rigid. Rotation data viewed in combination with strain data indicate that the joint is exhibiting rotational restraint stiffness of approximately 10% of the girder stiffness. This rotational restraint stiffness level was also confirmed numerically by evaluating the stiffness of the Number 16 reinforcing bars at 230 mm front and back crossing the joint between the top of the abutment and the backwall. Based on this evaluation and the measured behavior, numerical models were adjusted to allow full rotation at the girder–abutment connection which more closely models the actual condition than a rigid connection.

Girder Axial Force

Girder axial force was derived from monitored strains at midspan and near the abutment. Figs. 12(a and b) present 2D and 3D numerical model girder axial forces at midspan and at the north abutment superimposed on measurement based girder axial force (derived from strains) at the same locations. Numerical model response represents an average girder force due to minor nonsymmetries of the bridge and, therefore, the models. Graphs of measured response represent a best fit curve of data and an extrapolation to design temperatures of ±44°F.

Several factors contribute to the axial girder axial force, including abutment at-rest earth pressure, creep, and shrinkage, therefore, it is difficult to isolate a single load and response for measurement. Fig. 12(a) indicates a measured zero axial force magnitude at a temperature (approximately 16°C) similar to the numerical model zero load temperature. However, the extrapolated, measured axial force diverges significantly from girder to girder as well as from the numerical prediction of girder axial force, most significantly at temperatures above 32°C. This divergence is primarily due to the lack of measurement data at extreme temperatures. Near the abutment, Fig. 12(b)) indicates that there is a divergence of response between the numerical models and measured data at both the zero load point and more extreme temperatures. The measured response of Girders 1, 2, and 3 compare closely, however, Girder 4 appears to remain in tension. Girder axial force derived from 2D and averaged 3D numerical models match very closely at both midspan and the north abutment. It was noted that the range of axial force in the 3D model across girders was very wide due to temperature effects and influence of the deck. Based on observations and measured data, it is expected that tensile stresses under design level thermal loading alone range from 2.8 MPa to 5.5 psi. No cracks were observed in the deck or girders at the time these stresses were measured.

Summary and Conclusions

Objectives of this study included: (1) validating the use of *p-y* curves in developing multilinear soil springs to numerically model soil–pile interaction; (2) determining the effect of superstructure thermal loading and soil stiffness on pile predicted behavior; (3) establishing the mode of integral abutment movement; (4) determining the level of fixity at the girder–abutment connection; (5) ascertaining the influence of integral abutments on composite girder axial forces during thermal loading; and (6) determining the degree of accuracy obtained through level of analysis. Conclusions drawn from the present study include:

1. Development of multilinear soil springs from *p-y* curves to model soil–pile interaction in numerical models is a valid approach. This method eliminates many assumptions and numerous iterations that must be performed when using *COM624P* in combination with a structural finite element model incorporating linear soil springs to approximate soil–pile interaction.
2. Pile response determined using 2D and 3D numerical models is similar, therefore, accuracy derived from additional 3D modeling effort is not significant.
3. The primary mode of movement of the integral abutment is through rotation about the base of the abutment, not longitudinal displacement of the abutment, as typically assumed for design.
4. Field data indicate that the girder–abutment connection is not rigid and is best approximated as hinged. This was determined by observing that girder rotations are opposite of abutment rotations during bridge contraction and expansion.
5. Girder axial forces are influenced by the stiffness of the backfill during bridge expansion and by girder location within the bridge.
6. Creep and shrinkage may play a significant role in the axial response of the girders.
7. Girder tensile stress developed under thermal design temperature is significant and must be considered when designing prestressed girders.

Acknowledgments

This project was sponsored by Penn DOT and the Pennsylvania Transportation Institute.

References

American Association of State Highway and Transportation Officials, (AASHTO). (1989). "Thermal effects in concrete bridge superstructures." *NCHRP Rep. No. 276*, AASHTO, Washington, D.C.

Fennema, J. L. (2003). "Prediction and measured response of integral abutment bridges." Master of Science thesis, The Pennsylvania State Univ., University Park, Pa.

Lawver, A., French, C., and Shield, C. K. (2000). "Field performance of an integral abutment bridge." *Transportation Research Record. 1740*, Transportation Research Board, Washington, D.C., 108–117.

Oesterle, R. G., Refai, T. M., Volz, J. S., Scanlon, A., and Weiss, W. J. (1998). "Jointless and integral abutment bridges analytical research and proposed design procedures." *Rep. No. DTFH61-92-C-00154*, Federal Highway Administration, United States Department of Transportation, Washington, D.C.

Reese, L. C. (1985). "Behavior of piles and pile groups under lateral load." *Research Rep. No. FHWA/RD-85/106*, Federal Highway Administration, United States Department of Transportation, Washington, D.C.

Wang, S., and Reece, L. C. (1993). "COM624P-Laterally loaded pile analysis program for the microcomputer, Version 2.0." *Rep. No. FHWA-5A-91-048*, Office of Technology Applications, Federal Highway Administration, Washington, D.C.